Derivation of Tree Stem Curve and Volume Using Point Clouds

Abdul Nurunnabi [1,2], Felicia Teferle[1], Ana Novo[3], Jesús Balado[4], Emmett Ientilucci[5]

[1]Geodesy and Geospatial Engineering, Faculty of Science, Technology and Medicine, University of Luxembourg
6, rue Richard Coudenhove-Kalergi, L-1359 Luxembourg,− (abdul.nurunnabi, rebecca.teferle)@uni.lu
[2]Institute for Advanced Studies (IAS), University of Luxembourg, Luxembourg
[3]Forest Research Centre of Lourizán, Xunta de Galicia, 36080 Pontevedra, Spain,− ana.novo.gomez@xunta.gal
[4]CINTECX, GeoTECH Group, University of Vigo, 36310 Vigo, Spain,−jbalado@uvigo.es
[5]Chester F. Carlson Center for Imaging Science, Rochester Inst. of Technology, Rochester, USA, -Emmett@cis.rit.edu

Keywords: Biomass, Forest, Geometric Feature, Leaf-Wood Separation, Segmentation, Tree Information Modeling

Abstract

Developing a precise tree stem curve and robust estimation of stem volume are crucial for forest inventories with various applications. Laser scanned point clouds have been recognized as the most practical data for tree information modeling. Many methods for stem curve development involve estimating stem diameters at different heights and determining stem volume by utilizing fitted cylinders based on these diameters and the associated heights. The estimation of diameter depends on circle fitting. However, many circle fitting methods are non-robust and inaccurate in the presence of noise, outliers, and significant data gaps, resulting in faulty diameters and imprecise stem volume. Limited scanning, occlusions from the physical complexity, high tree density, and adjacent branches may cause data incompleteness, and generate outliers. To address these challenges, we employ robust statistical approaches to restrain the influence of outliers and data gaps. This paper contributes by (i) exploring the problems of robust diameter estimation for partial data, and in the presence of noise and outliers, (ii) understanding the impacts of using erroneous diameters in cylinder fitting, and later for stem curve and volume estimation, and (iii) developing a robust method that couples robust circle and cylinder fittings to derive precise stem curve and estimation of stem volume in the presence of outliers and partial data. We demonstrate the performance of the proposed algorithm through terrestrial laser scanning point clouds.

1. Introduction

Understanding tree structure, particularly the estimation of tree stem curve and volume (i.e., the total volume of the aboveground tree stem), is essential for characterizing forest stands and effectively managing forest resources. This encompasses quantifying logs, estimating aboveground biomass (AGB), and assessing carbon storage, all of which are crucial tasks for forest inventories (FIs) [Liang et al., 2018; Masuda et al., 2021; You et al., 2021; Abegg et al., 2023; Nurunnabi et al., 2024].

A stem curve is an arrangement of stem diameters that are a function of height. In Liang et al. (2018), it is defined as a set of stem diameters starting at the height of 0.65 meter (m) above the ground, followed by the diameters at breast height (DBH; at 1.3 m), and at every successive meter, such as at 2m, 3m, and so on, until the maximum measurable height around the treetop.

In conventional FIs, stem diameters are typically measured using slide callipers, measuring tapes and hypsometers, while tree volume is estimated using allometric models based on related measured parameters such as tree DBH and height (Akpo et al., 2021; Hyyppä et al., 2020; Yusup et al., 2023). However, measuring tree height and upper diameters physically can be time-consuming, laborious, and in some cases impossible, especially when dealing with trees exhibiting complex stem shapes or in densely populated and intertwined environments (Akpo et al., 2021; Masuda et al., 2021).

Light Detection and Ranging (LiDAR)-based non-invasive laser scanning systems provide three-dimensional (3D) point clouds (PCs) have been recognized as the most suitable data for tree information modeling (TIM) [Shu et al., 2022]. Terrestrial laser scanning (TLS) systems have gained popularity within forestry applications, and forest inventories (FIs), as TLS has become more affordable and manageable due to reductions in size and weight of associated hardware. This technology produces highly dense PCs, up to several million of points for a single tree. While PCs give detail geometry with high level of accuracy to present an object, processing them is not trivial as they are irregular, often incomplete, occluded by nearby complex structures, and contaminated with noise and outliers. Estimating tree stem volume from LiDAR PCs is an active area of contemporary research.

When estimating stem diameter and volume, particular consideration must be given to shadowing effects, especially when data are collected using a single scan. The most notable disadvantage of a single scan is the limited visibility of the stem caused by occlusion from surrounding branches, leaves, and nearby trees. This limitation can result in partial scans and data gaps, ultimately leading to lower-quality tree parameter estimation and characterization (Liang et al., 2018; Pueschel et al., 2013; Pitkänen et al., 2019). In contrast, multiple scans from various viewpoints around a tree can offer superior and comprehensive stem coverage. However, achieving accurate registration between scans in wide areas and complex environments may present challenges, as aligning all the points precisely can be difficult (Kawasaki and Masuda, 2022). Despite the advantage of generating a complete PC using multiple scans, the single-scan mode is often preferred due to its higher sampling efficiency (Pueschel et al., 2013).

A common approach for deriving stem profiles involves fitting a collection of geometric primitives, such as cylinders and circles, to a PC capturing the tree stem. Åkerblom et al. (2015) investigated various geometric primitives in quantitative structure models (QSMs) of tree stems and concluded that the circular cylinder is the most robust primitive. They found that it exhibits well-bounded volumetric modeling errors, even in the

presence of noise and data gaps. Most algorithms proposed for estimating DBH and stem profiles operate under the assumption that stem cross-sections are circular in shape. They typically reconstruct the stem as a series of circles or as portions of cylindrical or conical surfaces.

In this study, we focus more on incomplete data which may result because of a single scan. Consequently, there is a pressing need to develop methods capable of handling partial data in the presence of occlusions and outliers. To address the influence of outliers, occlusions, and partially scanned data on stem curve and volume estimation using LiDAR PCs, we propose a robust algorithm for deriving stem curves and stem volume estimation.

The remainder of the paper is organized into four sections. Section 2 provides a brief literature review. Section 3 outlines the methodology of the proposed algorithm. Section 4 evaluates the new algorithm through two experiments using real-world TLS datasets. Finally, Section 5 concludes the paper.

2. Related Literature

Over the years, numerous methods have been developed for characterizing tree stems. Two key aspects of this characterization are the stem curve, which represents stem diameters at different heights, and stem volume, defined as the cumulative wood volume of a stem. Typically, methods for estimating stem volume can be categorized into two groups: (i) destructive methods, which relies on felled trees, and (ii) non-destructive methods, based on standing trees (You et al., 2021).

The destructive approach entails extensive fieldwork, which is time-consuming and necessitates adherence to numerous strict rules and regulations. In a study conducted in the Amazonian Forest, Leão et al. (2021) found that a minimum of 29 to 81 sample trees were necessary, depending on tree species, to develop a reliable allometric model. Another destructive approach is the water displacement method, which entails immersing logs in a known quantity of water and measuring the subsequent increase in volume (Akossou et al., 2013). Conversely, the non-destructive approach is crucial for estimating tree growth and yield, thereby contributing to the decision-making process for sustainable forest management, the estimation of AGB, and carbon storage. Given our focus on remote sensing (RS) and the assessment of living trees, our primary concern lies with non-destructive approaches.

For standing trees, stem volume is typically calculated using allometric equations based on the tree's total height and DBH [Sumida et al., 2013]. Although DBH can be easily measured, estimating diameters for the upper part of the stem is challenging, and they may not accurately represent other parts of the stem. Kelly and Beltz (1987) conducted a comprehensive review of different regression models for tree volume estimation using DBH as a regressor variable. Consequently, many researchers utilize taper equations to estimate stem volume and diameter at various heights along the stem (Kozak, 2004; Poudel et al., 2018). However, proper selection of the allometric and/or taper equations is an analytical issue.

Typically, individual trees are extracted, and their stem shapes are estimated using circular and cylindrical approximation techniques (Masuda et al., 2021). Olofsson et al. (2014) employed a Hough Transformation (HT) [Duda and Hart, 1972] and a random sample consensus (RANSAC) [Fischler and Bolles, 1981]-based algorithm for tree stem classification and measurements. Their study concluded that the RANSAC algorithm effectively reduced noise and provided reliable estimates of tree stem parameters. In a similar vein, Wang et al. (2016) developed a method to model tree stems in an alpine landslide-affected forest. Their approach involved fitting a series of cylinders using a 2D-3D RANSAC-based method, demonstrating its applicability in challenging terrain conditions. In their 2017 study, Trochta et al. developed an open-source software application featuring a user-friendly graphical interface designed to compile algorithms for extracting tree parameters. This software enables the extraction of parameters such as DBH, tree height, stem curve, and volume. This algorithm employed a randomized HT (RHT) [Xu and Oja, 1993] for tree diameters estimation. Pitkänen et al. (2019) developed an automated processing chain wherein tree stems were modeled as cylinders. These models were subsequently utilized as prior information for a circle fitting procedure, taper curve estimation, and diameter calculation. Cabo et al. (2018) and later Prendes et al. (2021) improved an algorithm for tree height and diameter estimation using TLS data, consisting of four main steps: (i) height normalization, (ii) identification of stems, (iii) tree individualization, and (iv) calculation of stem diameters at different heights. To obtain stem diameters, the authors fit circles by minimizing the geometric error (i.e., the sum of squared distances from the points to the fitted circle) using the nonlinear least squares (Gauss-Newton) method (Gander et al., 1994) and Hyper (Al-Sharadqah and Chernov, 2009).

Bienert et al. (2014) developed a voxel-based technique to estimate tree volume of standing trees using TLS data. With recent advancements in computer vision and photogrammetry, particularly in the context of precision forestry, several recent studies have employed ground-based Structure from Motion (SfM) photogrammetry to analyze 3D tree structures (Piermattei et al., 2019). Hyyppa et al. (2020) developed an algorithm to derive stem curves using a pulse-based backpack laser scanner combined with an in-house simultaneous localization and mapping (SLAM) technique, along with a post-SLAM algorithm incorporating inclination angle correction. This methodology enabled to estimate stem volumes in boreal forest plots using the derived stem curves and tree heights. Windrim and Bryson (2020) developed a deep learning approach capable of isolating individual trees, identifying tree stem points, and constructing a segmented model of the main tree stem, which includes parameters such as tree height, diameter, taper, and sweep. Notably, their method relied on high-resolution airborne (helicopter) LiDAR PCs captured in two Radiata pine forests. Interested readers can refer to Ravaglia et al. (2019) for a comprehensive evaluation of three recent algorithms: STEP, CompuTree, and SimpleTree used for estimating stem DBH and diameters along the bole length.

3. Methodology

We propose a 7-step method for extracting tree stem curves and estimating stem volume. Our aim is to produce accurate diameters at different heights along the stem. This involves a fitting process for cross-sections of nearly circular (geometric) shapes obtained by dividing the stem into smaller vertical disks. Finally, cylinders are constructed based on the parameters of the robustly fitted circles formed by two consecutive disks, and the stem volume is estimated from the accumulated cylinders' volumes. The steps involved in the new algorithm are described in the following subsections and outlined by the flowchart depicted in Fig. 1.

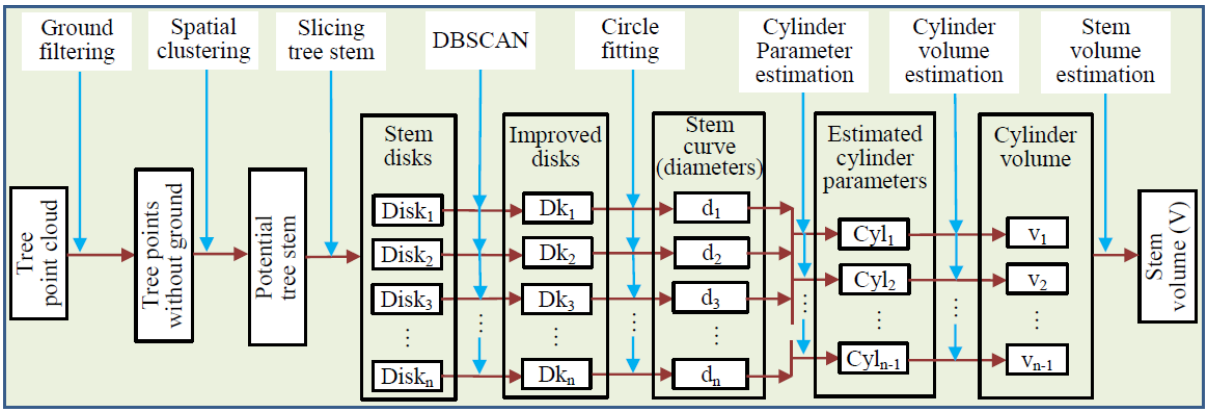

Figure 1. The flowchart of the proposed algorithm for tree stem curve and volume estimation. d_i = diameter for Dk_i (*i*th improved disk), Cyl_i= *i*th cylinder, v_i = volume of the Cyl_i, V = stem volume.

3.1 Step 1. Elimination of ground points

To analyze the tree stem, ground points associated with the tree should be eliminated. We employ a robust locally weighted regression (RLWR)-based ground filtering algorithm developed by Nurunnabi et al. (2016) to eliminate ground points. The method involves segmenting the dataset into convenient strips, applying the algorithm to each stripe, and then merging the results. For each strip, the algorithm operates on two 2D-orthogonal profiles: *x*-*z* and *y*-*z*. It follows an iterative process consisting of two main steps: (i) employing RLWR to achieve a robust nonlinear fit for the entire strip, and (ii) iteratively fitting each stripe while robustly down-weighting the *z* (elevation) values based on the residuals from the previous fit. This iterative process continues until it reaches the ground level. Ground points are defined as those falling within the lowest (ground) level, and the level with a threshold added to the ground level estimated via the repeated fits. This method demonstrates statistical robustness even in the presence of outliers. For further details, the reader is referred to Nurunnabi et al. (2016).

3.2 Step 2. Tree stem extraction and noise/outlier reduction

In this step, we want to reduce unnecessary branches and leaf points which come with the stem. Initially, as TLS data typically exhibit high density, we employ subsampling based on the underlying data density to mitigate accuracy bias stemming from heterogeneous data distribution, to reduce computational burden, and for having a consistent distance between adjacent points. This task potentially enhances clustering quality.

To reduce non-stem points from surrounding leaves and branches, we segment tree points using a region-growing-based clustering approach. Since trees lack regular shapes, we employ 3D Euclidean distance (ED)-based spatial clustering (EDSC). ED calculates one-to-one distances between nearby points. Region growing begins from a seed point with the lowest *z* value in the tree data. Points are accumulated within a predefined distance threshold, ED_{th}. Each new point serves as a subsequent seed point to search for other points until no point lies within the ED_{th} distance. A region containing a minimum number of points is identified as a cluster. The largest cluster, originating from the lowest point (matching with the ground level), is considered the potential tree stem. Additionaly, to reduce outlier effects, we can employ the noise and/or outlier reduction algorithm proposed in Nurunnabi et al. (2015).

3.3 Step 3. Slicing stem PC to get diameters

Following the definition of stem curve given in Liang et al. (2018), we need to find stem diameters at the heights of 0.65m, 1.3m, 2m, 3m, and so on. Hence, we slice the stem along its height (elevation, *z*) with a vertical length of 7cm at each height of (0.65±0.035)m, (1.3±0.035)m, (2±0.035)m, (3±0.035)m, and so forth, up to the measurable height. We call these 7cm slices (cross-sections), stem disks. Considering the data density, users can readjust the height of the disks. These disks serve the purpose of fitting circles and estimating diameters in subsequent steps. Users can alter the height (distance) between two consecutive disks according to the shape of the stem being studied. For a complex and irregular stem, it is advisable to consider the gaps between two disks as 0.5m instead of 1m.

3.4 Step 4. Improvement of stem disks

We project the 3D disk-points obtained from Step 3 onto the *x*-*y* (ground) plane to yield 2D points. To mitigate the influence of noise and outliers, especially when the outliers are significantly distant, we initially utilize DBSCAN (Density-Based Spatial Clustering of Applications with Noise), a machine learning algorithm introduced by Ester et al. (1996). DBSCAN is a nonparametric approach recognized for its ability to automatically identify clusters of diverse shapes and sizes, eliminating the need for a predetermined number of clusters. This density-based algorithm effectively groups closely situated points in a space, while discerning outliers as those significantly distanced from the clusters, often residing solitarily or scattered within low-density areas. As a result, one of DBSCAN's key strengths lies in its resilience to noise and outliers, this makes it particularly suitable for datasets characterized by irregular shapes and fluctuating densities. Fig. 2(b) demonstrates the application of DBSCAN.

3.5 Step 5. Circle fitting and diameter estimation

The 2D points may still contain outliers, particularly those originating from surrounding branches, leaves, and loose barks, which can manifest as scattered and/or clustered outliers. Furthermore, some of the disks may be incomplete due to limited scanning, resulting in data gaps, especially in cases where data are collected through a single scan. Fitting circles to incomplete data and in the presence of outliers poses a significant challenge. The widely used least squares fitting-based geometric approach is highly sensitive to outliers. We are inspired by the robust circle fitting introduced by Nurunnabi et al. (2018). For the circle fitting procedure, we adopt 'Hyper' (Al-Sharadqah and Chernov, 2009), an algebraic fitting method that satisfies many essential mathematical properties. The authors assert that their technique surpasses many existing algebraic methods, achieving circle fitting accuracy comparable to geometric fitting and even yielding superior results for partial circular arcs. However, as shown in Fig. 2(c), it is evident that even such an efficient circle

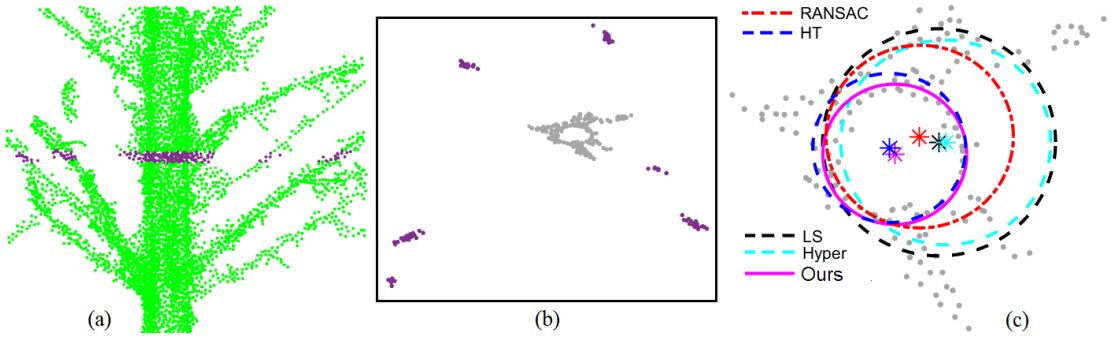

Figure 2. (a) A part of a tree stem, (b) projection of a 3D stem disk [purple color in (a)] onto a 2D plane; purpole points are identified as outlying points, (c) fitted circles to the inlier points [ash color in (b)] by using RANSAC, HT, LS, Hyper and our method.

fitting method (Hyper) is not immune to outlier effects, as we see here the fitted circle is significantly biased towards the outliers. In the literature reviw of Section 2, we noticed that, many algorithms used RANSAC, HT, Hyper or least squares. We perfomed all of them on our dataset [(ash color points in Fig. 2(b)]. Fig. 2(c) demonstrates that neither RANSAC, HT, Hyper, nor the least squares methods are immune to the influence of outliers. Hence, to reduce the outlier effects, especially for cluster outliers, Hyper is coupled with the repeated least trimmed squares (RLTS) regression (Rousseeuw and Leroy, 2003). Initially, we fit a cirle with the Hyper and then utilize RLTS. LTS is a robust regression technique, is designed to minimize the influence of outliers in the dataset, RLTS proceeds by identifying outliers and fits iteratively and downweighting the most outlying observations. It finds outliers and then assigns weights to the outliers according to their degree of outlyingness. It minimizes the sum of the weighted squared residuals:

$$minimize_{(C,R)} \sum_{i=1}^{n} w_i r_i^2, \quad (1)$$

where $C\ (a_x,\ b_y)$ and R is the centre and radius of the fitted circle, respectively. We fix $w_i = 0$ when the ith point is an outlier, otherwise $w_i = 1$, and the ith residual is defined as:

$$r_i = \sqrt{(p_{ix} - a_x)^2 + (p_{iy} - b_y)^2} - R = d_i - R, \quad (2)$$

where $p_{i(x,y)}\ \ (i = 1, 2, \dots, n)$ is the ith point. The circle fitting process starts with a minimal subset of (usually 3) points. Monte Carlo (MC) type probabilistic principle (c.f., Fischler and Bolles, 1981; Rousseeuw and Leroy, 2003) is employed to have an outlier free initial subset, and to determine the number of iteration (I_n) required for getting the outlier free subset. The circle fitting process works as: (i) fits circle based on an intial random subset, (ii) based on the fit, calculates the residuals for all the data points, (iii) arrange the points in ascending order according to their residual values, (iv) finds first h points ($h = \lceil 0.5n \rceil$), and (v) fits a circle based on the h points, and finally (vi) organizes the data in ascending order according to the resudal values from the latest fit, and sum up the residuals until the h points, put the sum values in a list. These six (i-vi) tasks are repated I_n times. After performing all the repetitions, we select the h subset of points for which the sum of residuals is the lowest, and the fit based on that subset is the final one. The resltant redius is used to calculate the diameter of the fitted circle.

3.6 Step 6. Stem curve derivation and cylinder parameters estimation

We derive the tree stem curve based on stem diameters estimated at various positions using circle fitting as described in Step 5. We then employ a standard method to fit cylinders using two diameters estimated from successive disks.

Given the typical morphology of a tree stem, it is reasonable to assume that the diameters at the two ends of a section may differ, typically the upper end diameter smaller than the lower end, suggesting a conical cylinder (frustum) shape, see Fig. 3. To reconstruct such a conical cylinder based on the diameters of the two ends, we proceed to determine the parameters: the cylinder axis, radii at both ends, and the length of the cylinder. In the initial step, we identify the cylinder axis by establishing the line passing through the centers of the two consecutive circles, which represent the ends of the cylinder. Thus, the line connecting the centers of the circles represents the cylinder axis. Once the axis is established, the length of the cylinder (i.e., the length of the axis) can be calculated as the distance between the centers of the two given circles.

3.7 Step 7. Stem volume estimation

We calculate the volume (v) of each fitted cylinder based on two diameters and the distance between two successive disks, using the formula defined in Eq. (3) [Bienert et al., 2014; Åkerblom et al., 2015]. Then, we sum the volumes of all (n-1) cylinders to obtain the required stem volume (V), Eq. (4).

$$v = \pi h \left(\frac{r_1^2 + r_2^2 + r_1 r_2}{3} \right), \quad (3)$$

$$V = v_1 + v_2 + \cdots + v_{n-1}, \quad (4)$$

where r_1 and r_2 are the two raddi at the ends of the cylinder, and h is the estimated height of the cylinder, as seen in Fig. 3. .

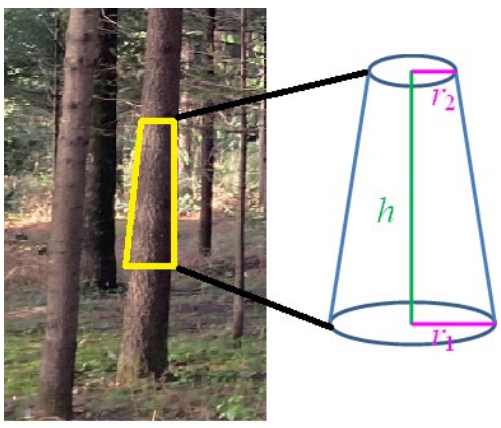

Figure 3. Part of a tree stem shows a conical cylindrical shape.

4. Experiments, Evaluation, and Discussion

In this section, we present two experiments utilizing real-world TLS data. To facilitate comparison with existing methods, we implemented the 3D Forest and 3DFin (3D Forest Inventory) software. These tools derive tree stem curves using methodologies proposed by Trochta et al. (2017), and Cabo et al. (2018) and Prendes et al. (2021), respectively. As mentioned in Section 2, Trochta et al. (2017) employed the randomized Hough transform (RHT) [Xu and Oja, 1993], known for its robustness in circle fitting. In 3DFin, circle fitting is based on an improved version of Cabo et al. (2018)'s approach utilizing the least squares method with Hyper (Al-Sharadqah and Chernov, 2009). Notably, in our algorithm, we further employ Hyper alongside RLTS to mitigate outlier effects during circle fitting when points having significant data gap.

4.1 Experiment 1

For the first experiment, we took a Scots pine (*Pinus sylvestris*) tree from Weiser et al. (2022). The data were collected using a RIGEL VZ-400 based TLS system. The tree depicted in Fig. 4(a) lacked ground points and consisted of 1,198,381 points with a height and DBH of 30.7m and 48.5cm, respectively. We downsampled the data with a spacing of 0.03m and applied EDSC ($ED_{th} = 0.04$) to extract the potential tree stem. The results created the largest segment shown in Fig. 4(b), representing the tree stem, with most branches and leaves removed. We then divided the stem into *n* segments, each with a vertical length of 7cm, starting at height of 0.65m, then at 1.3m, 2m, 3m, and so forth, until reaching the feasible height around 25m. This process yielded 28 (*n*) disks, each projected distinctly onto the *x*-*y* plane. We performed DBSCAN to remove outliers that are significantly distant from the main circular portion created by the disks. Now, circles were fitted for each of the 2D datasets. The results yielded the necessary diameters for the stem curve shown as magenta circles in Fig. 4(b). To facilitate comparison, we implemented 3D Forest and 3DFin. The results are detailed in Table 1, and visually exposed in Fig. 4. The estimated DBHs for 3D Forest (48.6cm) and our method (48.7cm) are nearly equal and close to the provided ground truth of 48.5 cm. For 3DFin, it was underestimated to 47.1 cm. At a height of 19m, the estimated diameters are 48.6cm, 28.7cm, and 30.9cm for 3D Forest, 3DFin, and our method, respectively. As depicted in Fig. 4(g), at 19m height , RHT (3D Forest; Trochta et al., 2017) overestimated by 20.6cm (where the expected diameter is around 28cm) due to the outliers in the maroon rectangles. In Fig. 4(f), 3D Forest fixed the diameter almost the same as ours, but both 3D Forest and 3DFin are significantly displaced towards the outliers. Figs. 4(f) and (g) illustrate that 3DFin and 3D Forest encounter challenges in fitting robust circles due to outlier contamination and incomplete data, whereas our method precisely fits the circles, enabling us to derive the stem curve accurately. Figs. 4(c) and (d) reveal that Cabo et al. (2018) [3DFin] and Trochta (2017) [3D Foreest] failed to derive the stem curve until the top height; they could estimate diameters only until 19m and 20m, respectively, while our method develops the stem curve up to 25m [Fig. 4(b)]. For 3D Forest, the algorithm halts when the estimated diameter exceeds twice the diameter of both of the two previous circles, which is a limitation to get diameter until the tree top.

In Fig. 5 (line diagram) and Table 1, we consistently observe decreasing diameters toward the treetop, smoothly fitted at various heights using our method, displaying a more even trend than 3D Forest and 3DFin. Certainly, the existing methods produce imprecise stem volume. In conclusion, we construct cylinders based on the diameters of adjacent circles and related heights, estimating the stem volume to be 2.50m^3. Whereas, 3D Forest and 3DFin produce stem volumes of 2.38m^3 and 2.23m^3, respectively.

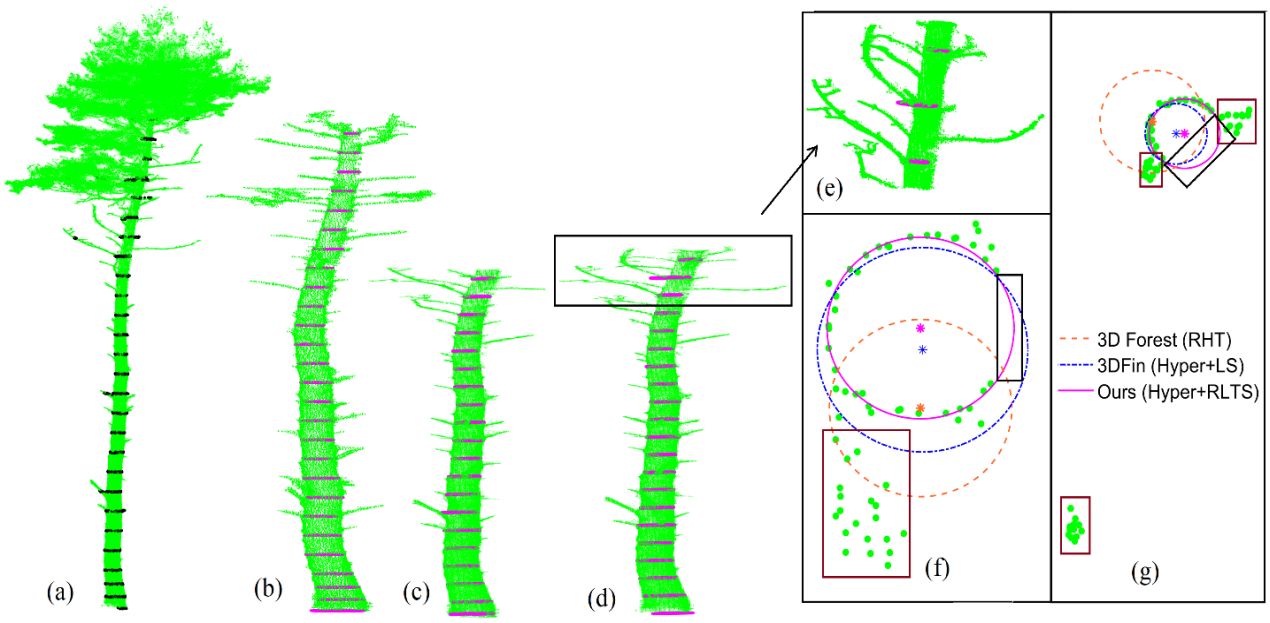

Figure 4. (a) Scots pine tree point cloud, black rings indicating stem disk-circles to be fitted at those heights, (b) the stem segment obtained through spatial clustering, magenta rings representing the fitted circles (stem curve; our method) at defined heights, (c) stem curve derived by 3DFin (d) stem curve derived by 3D Forest, (e) a part of the stem curve from Fig. (d); with fitted circles (magenta rings) at 18m, 19m, and 20m, (f) fitted circles at 18m height; the blank space in the black box represents an incomplete circular arc, (g) fitted circles at 19m height, points in the maroon rectangles showing the presence of clustered and scattered outliers.

Height/position at (m)		0	0.65	1.0	**1.3**	2	3	4	5	6	7	8	9	10	11
Dia-meter (cm)	3DForest (RHT)	50.2	-	50.8	**48.6**	45.2	43.8	41.0	45.8	40.6	40.4	37.6	36.6	40.8	35.4
	3DFin (Hyper)	55.0	51.3	50.5	**47.1**	45.1	43.1	41.4	45.7	46.4	41.2	40.4	36.3	37.3	36.9
	Ours	60.3	52.5	50.5	**48.7**	44.7	43.8	41.1	41.6	41.0	40.2	37.7	36.4	36.8	36.3
Height/position at(m)		12	13	14	15	16	17	18	**19**	20	21	22	23	24	25
Dia-meter (cm)	3DForest (RHT)	36.2	33.0	35.4	31.0	30.8	29.0	28.8	**48.6**	27.2	-	-	-	-	-
	3DFin (Hyper)	34.3	35.1	32.8	33.4	31.6	30.9	33.2	**28.7**	-	-	-	-	-	-
	Ours	36.0	34.0	34.2	32.3	29.8	28.9	28.5	**30.9**	27.5	27.1	25.7	24.1	23.4	17.5

Table 1. Estimated diameters w. r. t. the corresponding heights of the stem curves at Fig. 4(b), (c), (d). Ground truth DBH is 48.5cm.

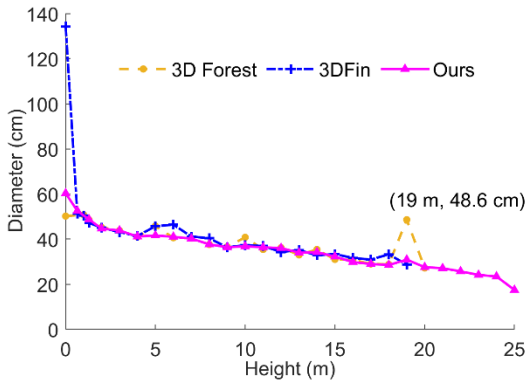

Figure 5. Line diagram for estimated diameters versus different heights along the stem for the Scots pine tree.

4.2 Experiment 2

For the second experiment, we chose an additional TLS dataset of a Douglas-fir (*Pseudotsuga menziesii*) tree captured using a RIGEL VZ-400 scanner, detailed in Weiser et al. (2022). The tree data depicted in Fig. 6(a) comprises 2,559,351 points, with a height of 39.3m and a DBH of 48.2cm.

We downsampled the data using the same spacing (0.03 m) as for the previous experiment. To eliminate unnecessary branches and leaves, we utilized EDSC with an ED_{th} value of 0.04m, resulting in the extraction of the potential stem segment, approximately 32m in height, as depicted in Figure 6(b). Subsequently, we sliced the stem to generate stem disks with a vertical length of 7cm at intervals, starting from a height of ground level (0.0m), and continuing at 0.65m, 1.3m, 2m, 3m, and so forth, until reaching approximately 32m. These disks were projected onto the *x-y* plane, where DBSCAN was employed to remove distant outliers not constituting stem points. Finally, circles were fitted to each of the 2D point sets generated by the stem disks. We implemented 3D Forest and 3DFin. The estimated stem diameters at different heights are presented in Table 2. The resulting diameters are illustrated as the stem curve, depicted by orange, blue and magenta circles, visually shown in Figs. 6 (c), (d), and (e). We observed that 3D Forest, 3DFin, and our method could generate diameters up to 11m, 29m, and 32m, respectively, with our method being capable of generating the stem curve at the highest point. Upon visual examination of the raw data, we comprehended that beyond 32 meters, the tree lacks significant wood structure in the form of a stem. We estimated the DBH to be 48.3cm, which is the closest to the ground truth DBH of 48.2cm. However, for 3D Forest, it was overestimated at 49.0cm, and for 3DFin, it was underestimated at 47.5cm. At the heights of 28m and 29m, 3DFin estimated diameters of 41.9cm and 28.1cm, respectively, with the diameter of 41.9cm being inflated almost double of the diameter (21.8cm) at 27m. In contrast, our method estimated diameters of 21.3cm and 19.7cm for the same heights.

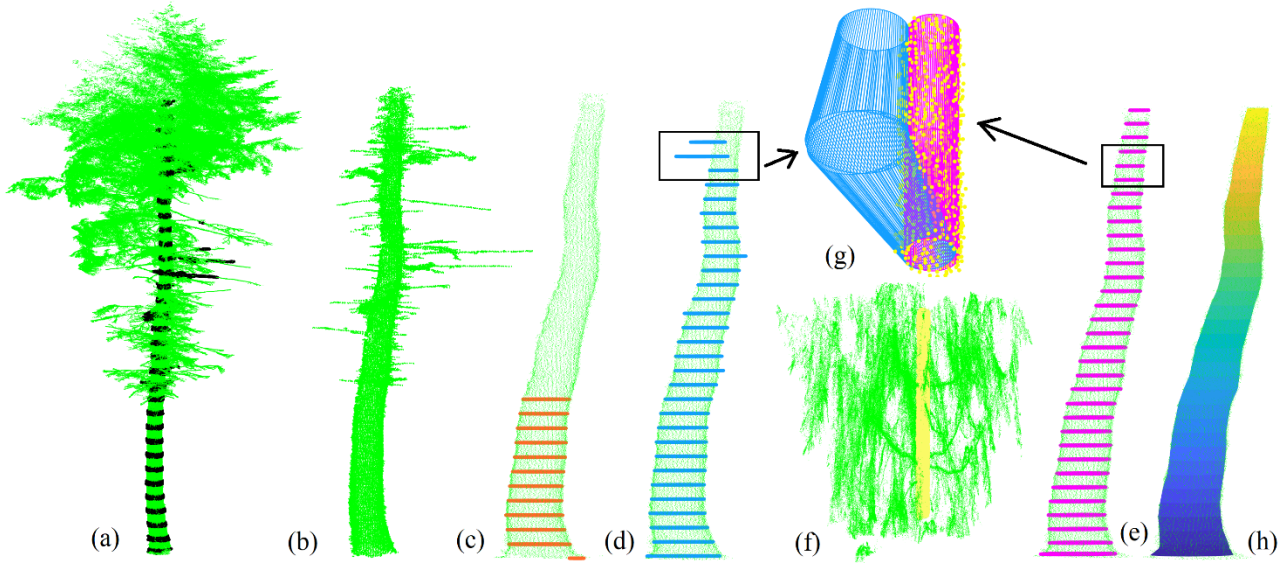

Figure 6. (a) Douglas-fir tree point cloud, black points (look rings) indicating specific positions where circles to be fitted for getting stem diameters, (b) extracted stem segment obtained by using spatial clustering, (c) stem curve (orange rings) using 3D Forest; rings representing the fitted circles at different heights, (d) stem curve (blue rings) by using 3DFin, (e) stem curve (magenta rings) by using our method, (f) tree point cloud between 27m to 29m, (g) two fitted cylinders by using 3DFin and our method for the stem part (yellow points) in Fig. (f), (h) reconstructed stem using the fitted cylinders based on our method.

https://doi.org/10.5194/isprs-archives-XLVIII-4-W11-2024-81-2024

Height/position at (m)		0	0.65	1.0	**1.3**	2	3	4	5	6	7	8	9
Dia-meter (cm)	3D Forest (RHT)	11.8	-	49.0	**49.0**	46.0	45.4	42.8	42.0	41.0	40.6	40.0	38.8
	3DFin (Hyper)	58.6	50.7	47.9	**47.5**	45.3	44.1	42.5	41.9	40.8	39.9	40.1	38.8
	Ours	59.6	51.1	49.2	**48.3**	45.6	45.1	43.0	42.2	40.7	40.2	39.9	38.6
Height/position at(m)		10	11	12	13	14	15	16	17	18	**19**	20	21
Dia-meter (cm)	3D Forest (RHT)	38.0	37.2	-	-	-	-	-	-	-	-	-	-
	3DFin (Hyper)	38.3	37.3	36.9	38.9	37.2	35.3	35.7	35.5	32.5	**31.7**	29.5	32.9
	Ours	37.9	37.9	38.9	36.0	34.7	34.2	33.3	32.7	31.8	**30.6**	29.3	28.5
Height/position at(m)		22	23	24	25	26	27	**28**	**29**	30	31	32	
Dia-meter (cm)	3D Forest (RHT)	-	-	-	-	-	-	-	-	-	-	-	
	3DFin (Hyper)	29.2	26.6	27.0	24.4	25.2	21.8	**41.9**	**28.1**	-	-	-	
	Ours	27.3	26.4	25.2	24.8	23.1	21.8	**21.3**	**19.7**	19.2	17.4	15.2	

Table 2. Estimated diameters w. r. t. the corresponding heights of the stem curves at Fig. 6(c), (d), (e). Ground truth DBH is 48.2cm.

The line diagram in Fig. 7 and Table 2 illustrate that our method estimated diameters at various heights, displaying a smooth decreasing trend towards the treetop and showing a more even pattern compared to 3D Forest and 3DFin. In conclusion, we fitted cylinders with accurate length and radii using the adjacent circles from the respective stem disks, estimating the stem volume to be 2.89m³. In contrast, RHT-based 3D Forest and Hyper-based 3DFin estimated stem volumes of 1.46m³ and 3.05m³, respectively. Fairly, both the estimates are inaccurate.

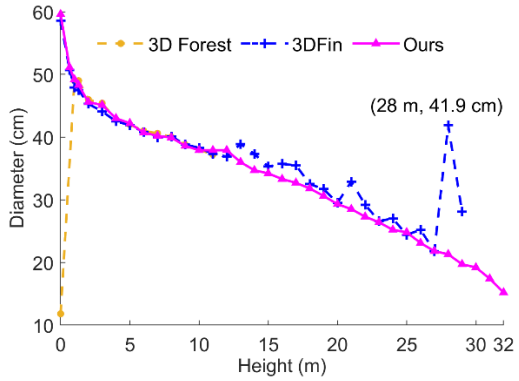

Figure 7. Line diagram for estimated diameters versus different heights along the stem for the Douglas-fir tree.

5. Conclusions

In this paper, we present a robust method for deriving tree stem curve and estimating stem volume using LiDAR point clouds. Our algorithm employs robust circle fitting to estimate tree diameters at various heights along the stem. Specifically, it utilizes Hyper, an algebraic circle fitting approach coupled with robust RLTS regression. This approach offers advantages in handling outliers and addresses significant portion of data gaps, which may result in incomplete circular arcs. The algorithm derives cylinder parameters using the fitted diameters/radii of the respective circles and the length measured between the consecutive centers of the fitted circles. Using clustering approaches (EDSC and DBSCAN), the new method successfully separates unwanted tree branches and leaves from the target tree and/or nearby trees. Moreover, this method precisely estimates stem volume even when the tree stem is not perfectly straight, as it fits irregular cylinder shapes with improved cylinder fit matching within an adjustable (smaller or larger) region of the tree stem. The distance between consecutive disks can be adjusted, ranging from 1m to less than or greater than 1m, for example, 0.5m or 2m, based on the underlying tree stem structure.

The method is indeed independent of tree species and size, providing adaptability across diverse forest environments. However, it's worth noting that this algorithm may necessitate additional processing time due to its iterative nature. In future research, efforts will be directed towards optimizing the process, with a focus on enhancing automation and efficiency to reduce processing time, especially considering its application for forest stand analysis having complex environment.

Acknowledgement

Abdul Nurunnabi is funded through the IAS-AUDACITY-PIONEER-2022 project at the University of Luxembourg.

References

Abegg, M., Ruedi Bösch, R., Kükenbrink, D., Morsdorf, F., 2023. Tree volume estimation with terrestrial laser scanning — Testing for bias in a 3D virtual environment. *Agric For Meteorol.*, 331, 109348, 1–15.

Åkerblom, M., Raumonen, P., Kaasalainen, M., Casella, E., 2015. Analysis of geometric primitives in quantitative structure models of tree stems. *Remote Sens.*, 7(4), 4581–4603.

Akossou, A. Y., Arzouma, S., Attakpa, E. Y., Fonton, N. H., Kokou, K., 2013. Scaling of teak (Tectona grandis) logs by the xylometer technique: accuracy of volume equations and influence of the log length. *Diversity*, 5(1), 99–113.

Akpo, H.A., Atindogbé, G., Obiakara, M.C., Adjinanoukon, A.B., Gbedolo, M, Fonton, N.H., 2021. Accuracy of common stem volume formulae using terrestrial photogrammetric point clouds: a case study with savanna trees in Benin. *J. For. Res.*, 32, 2415–2422.

Al-Sharadqah, A., Chernov, N., 2009. Error analysis for circle fitting algorithms. *Electron. J. Stat.*, 3, 886–911.

Bienert, A., Hess, C., Maas, H.G., Von Oheimb, G., 2014. A voxel-based technique to estimate the volume of trees from terrestrial laser scanner data. *Int. Arch. Photogramm. Remote Sens. Spatial Inf. Sci.*, 40, 101–110.

Cabo, C., Del Pozo, S., Rodríguez-Gonzálvez, P., Ordóñez, C., González-Aguilera, D., 2018. Comparing terrestrial laser scanning and wearable laser scanning for individual tree modeling at plot level. *Remote Sens.*, 10(4), 540.

Duda, R. O., Hart, P. E., 1972. Use of the Hough transformation to detect lines and curves in pictures. *Commun. ACM*, 15(1), 11,15.6.

Ester, M., Kriegel, H. P., Sander, J., Xu, X., 1996. A density-based algorithm for discovering clusters in large spatial databases with noise. In *KDD*, 96(34), 226–231.

Fischler, M. A., Bolles, R. C., 1981. Random sample consensus: a paradigm for model fitting with applications to image analysis and automated cartography. *Commun. ACM*, 24(6), 381–395.

Gander, W., Golub, G. H., Strebel, R., 1994. Least-squares fitting of circles and ellipses. *BIT Numer. Math.*, 34, 558-578.

Hyyppä, E., Kukko, A., Kaijaluoto, R., White, J.C., Wulder, M.A., Pyörälä, J., Liang, X., et al., 2020. Accurate derivation of stem curve and volume using backpack mobile laser scanning. *ISPRS J Photogramm and Remote Sens.*, 161, 246–262.

Kawasaki, H., Masuda, H., 2022. Accurate Calculation of Tree STEM Traits in Forests by Local Correction of Point Cloud Registration. *Int. Arch. Photogramm. Remote Sens. Spatial Inf. Sci*., 43, 209–214.

Kelly, J. F., Beltz, R. C., 1987. A comparison of tree volume estimation models for forest inventory. *United States Department of Agriculture, Forest Service, Southern Forest Experiment Station*, 233.

Kozak, A., 2004. My last words on taper equations. *For. Chron.*, 80(4), 507–515.

Leão, F. M., Nascimento, R. M., Emmert, F., Santos, G. G. A., Caldeira, N. A. M., et al., 2021. How many trees are necessary to fit an accurate volume model for the Amazon Forest? A site-dependent analysis. *For. Ecol. Manag.*, 480, 118652.

Liang, X., Hyyppä, J., Kaartinen, H., Lehtomäki, M., Pyörälä, J., Pfeifer, N., et al., 2018. International benchmarking of terrestrial laser scanning approaches for forest inventories. *ISPRS J. Photogramm. Remote Sens*., 144, 137–179.

Masuda, H., Hiraoka, Y., Saito, K., Eto, S., Matsushita, M., Takahashi, M., 2021. Efficient calculation method for tree stem traits from large-scale point clouds of forest stands. *Remote Sens.*, 13(13), 2476.

Nurunnabi, A., West, G., Belton, D., 2015. Outlier detection and robust normal-curvature estimation in mobile laser scanning 3D point cloud data. *Pattern Recognit*., 48(4), 1404–1419.

Nurunnabi, A., West, G., Belton, D., 2016. Robust locally weighted regression techniques for ground surface points filtering in mobile laser scanning three-dimensional point cloud data. *IEEE Trans Geosci Remote Sens.*, 54(4), 2181–2193.

Nurunnabi, A., Sadahiro, Y., Laefer, D., 2018. Robust statistical approaches for circle fitting in laser scanning three-dimensional point cloud data. *Pattern Recognit*, 81, 417–431.

Nurunnabi, A., Teferle, F., Laefer, D., Chen, M., Ali, M. M., 2024. Development of a Precise Tree Structure from LiDAR Point Clouds. *ISPRS Technical Commission II Symposium*, June 11-14, 2024, Las Vegas, Nevada, USA.

Olofsson, K., Holmgren, J., Olsson, H., 2014. Tree stem and height measurements using terrestrial laser scanning and the RANSAC algorithm. *Remote Sens*., 6(5), 4323–4344.

Pitkänen, T.P., Raumonen, P., Kangas, A., 2019. Measuring stem diameters with TLS in boreal forests by complementary fitting procedure. *ISPRS J Photogramm and Remote Sens*., 147, 294–306.

Piermattei, L., Karel, W., Wang, D., Wieser, M., Mokroš, M., Surový, P., et al., 2019. Terrestrial structure from motion photogrammetry for deriving forest inventory data. *Remote Sens*., 11(8), 950.

Poudel, K. P., Temesgen, H., Gray, N., 2018. Estimating upper stem diameters and volume of Douglas-fir and Western hemlock trees in the Pacific northwest. *Forest Ecosystems*, 5, 1–12.

Prendes, C., Cabo, C., Ordoñez, C., Majada, J., Canga, E., 2021. An algorithm for the automatic parametrization of wood volume equations from Terrestrial Laser Scanning point clouds: application in Pinus pinaster. *GIScience & Remote Sensing*, 58(7), 1130–1150.

Pueschel, P., Newnham, G., Rock, G., Udelhoven, T., Werner, W., Hill, J., 2013. The influence of scan mode and circle fitting on tree stem detection, stem diameter and volume extraction from terrestrial laser scans. *ISPRS J Photogrammetry and Remote Sens*., 77, pp.44–56.

Ravaglia, J., Fournier, R.A., Bac, A., Véga, C., Côté, J.F., Piboule, A., Rémillard, U., 2019. Comparison of three algorithms to estimate tree stem diameter from terrestrial laser scanner data. Forests, 10(7), 599.

Rousseeuw, P. J., Leroy, A. M., 2003. *Robust Regression and Outlier Detection*. John Wiley & Sons.

Sumida, A., Miyaura, T., Torii, H., 2013. Relationships of tree height and diameter at breast height revisited: analyses of stem growth using 20-year data of an even-aged Chamaecyparis obtusa stand. *Tree Physiol.*, 33(1), 106–118.

Shu, Q., Rötzer, T., Detter, A., Ludwig, F., 2022. Tree information modeling: a data exchange platform for tree design and management. *Forests*, 13(11), 1955.

Trochta, J., Krůček, M., Vrška, T., Král, K., 2017. 3D Forest: An application for descriptions of three-dimensional forest structures using terrestrial LiDAR. PloS one, 12(5), 1–17.

Wang, D., Hollaus, M., Puttonen, E., Pfeifer, N., 2016. Automatic and self-adaptive stem reconstruction in landslide-affected forests. *Remote Sens*., 8(12), 974.

Weiser, H., Schäfer, J., Winiwarter, L., Krašovec, N., Fassnacht, F. E., Höfle, B., 2022. Individual tree point clouds and tree measurements from multi-platform laser scanning in German forests. *Earth Syst. Sci. Data*, 14(7), 2989–3012.

Windrim, L., Bryson, M., 2020. Detection, segmentation, and model fitting of individual tree stems from airborne laser scanning of forests using deep learning. *Remote Sens*., 12(9), 1469.

Xu, L., Oja, E., 1993. Randomized Hough Transform (RHT): Basic mechanisms, algorithms, and computational complexities. *CVGIP: Image Understanding*, 57(2), 131–154.

You, L., Wei, J., Liang, X., Lou, M., Pang, Y., Song, X., 2021. Comparison of numerical calculation methods for stem diameter retrieval using terrestrial laser data. *Remote Sens*., 13(9), 1780.

Yusup, A., Halik, Ü., Keyimu, M., Aishan, T., Abliz, A., et al., 2023. Trunk volume estimation of irregular shaped Populus euphratica riparian forest using TLS point cloud data and multivariate prediction models. *For. Ecosyst*., 10, 100082.